ISSN 1674-1056
http://cpb.iphy.ac.cn
http://iopscience.iop.org/cpb
中国物理 B
Chinese Physics
中国物理
Chinese Physics B

Coordinated chaos control of urban expressway based on synchronization of complex networks

Ming-bao Pang(庞明宝), Yu-man Huang(黄玉满)

Citation: Chin. Phys. B . 2018, 27(11): 118902. **doi:** 10.1088/1674-1056/27/118902
Journal homepage: http://cpb.iphy.ac.cn; http://iopscience.iop.org/cpb

What follows is a list of articles you may be interested in

Model and application of bidirectional pedestrian flows at signalized crosswalks

Tao Zhang(张涛), Gang Ren(任刚), Zhi-Gang Yu(俞志钢), Yang Yang(杨阳)

Chin. Phys. B . 2018, 27(7): 078901. **doi:** 10.1088/1674-1056/27/7/078901

Effects of rainy weather on traffic accidents of a freeway using cellular automata model

Ming-Bao Pang(庞明宝), Bo-Ning Ren(任泊宁)

Chin. Phys. B . 2017, 26(10): 108901. **doi:** 10.1088/1674-1056/26/10/108901

A new cellular automata model of traffic flow with negative exponential weighted look-ahead potential

Xiao Ma(马骁), Wei-Fan Zheng(郑伟范), Bao-Shan Jiang(江宝山), Ji-Ye Zhang(张继业)

Chin. Phys. B . 2016, 25(10): 108902. **doi:** 10.1088/1674-1056/25/10/108902

Influence of bus stop with left-turn lines between two adjacent signalized intersections

Ming-Bao Pang(庞明宝), Lan-Hang Ye(叶兰杭), Ya-Nan Pei(裴亚男)

Chin. Phys. B . 2016, 25(8): 088901. **doi:** 10.1088/1674-1056/25/8/088901

A cellular automata model of traffic flow with variable probability of randomization

Zheng Wei-Fan, Zhang Ji-Ye

Chin. Phys. B . 2015, 24(5): 058902. **doi:** 10.1088/1674-1056/24/5/058902

Coordinated chaos control of urban expressway based on synchronization of complex networks*

Ming-bao Pang(庞明宝)† and Yu-man Huang(黄玉满)‡

School of Civil and Transportation, Hebei University of Technology, Tianjin 300401, *China*

(Received 2 June 2018; revised manuscript received 15 August 2018; published online 19 October 2018)

We investigate the problem of coordinated chaos control on an urban expressway based on pinning synchronization of complex networks. A node coupling model of an urban expressway based on complex networks has been established using the cell transmission model (CTM). The pinning controller corresponding to multi-ramp coordinated controller was designed by using the delayed feedback control (DFC) method, whose objective is to realize periodical orbits from chaotic states. The concrete pinning control nodes corresponding to the subsystems of regulating the inflows from the on-ramps to the mainline were obtained and the parameters of the controller were optimized by using the stability theory of complex networks to ensure the network synchronization. The validity of the proposed coordinated chaos control method was proven via the simulation experiment. The results of the examples indicated that the order motion on urban expressway can be realized, the wide-moving traffic jam can be suppressed, and the operating efficiency is superior to that of the traditional control methods.

Keywords: pinning synchronization of complex networks, multi-on-ramp metering of urban expressway, chaos control, delayed feedback control (DFC)

PACS: 89.40.Bb, 89.40.–a, 89.75.Fb **DOI:** 10.1088/1674-1056/27/11/118902

1. Introduction

In China, traffic networks, especially urban expressways, have reached a high level of jamming. Congestion is known to reduce the nominal capacity of the network infrastructure and has a serious impact on travel time, traffic safety, fuel consumption, and environmental pollution.[1–3] Various traffic management measures, especially multi-on-ramp coordinated control, have recently have been proposed to control the urban expressway.[4,5] This aims to improve the traffic conditions of urban expressway by appropriately regulating the inflows from the on-ramps to the mainline. Traditionally, there are four types of coordinated control algorithms: integrated ramp control algorithms, feedback control algorithms, heuristic coordinated control algorithms, and large scale system decomposition and coordination algorithm.[6,7] For example, the coordinated control strategy (CORDIN) is based on a heuristic approach.[8] The main philosophy of this strategy consists of using free upstream on-ramp capacities in case of downstream motorway congestion. However, there are some limitations in these studies. First, synchronization and pinning control of traffic flow on urban expressway have not been discussed by using complex networks theory, although their nonlinear behaviors and complexity, including dynamical evolution, topological structure, connection or node diversity, meta-complication, and so on, have been proven in some literature.[9] Second, the coordinated control section of an urban expressway is predetermined by the researchers or traffic managers and all on-ramps in the control section are inputted to the control signal if the section needed control. This is a problem for the expanded control section or increasing the number of on-ramps makes many vehicles that want to travel on urban expressway have to queue on the on-ramps or travel on those ordinary urban streets. The traffic jams phenomena on ordinary urban streets will become more serious and the goal of high operating efficiency on an expressway cannot be achieved. At the same time, it makes a social inequity problem for the road users. If we decrease the control sections or on-ramp metering number, then the wide-moving traffic jamming phenomena cannot be suppressed rapidly and the operating efficiency of expressway can decline. These are not the original intentions of traffic control. So the first step of coordinated control is to determine the on-ramps that the inflows should be regulated. Third, few approaches are related to chaos control of traffic flow.

The nonlinear dynamic behavior of traffic flow has been studied by many researchers.[10] Traffic flow on road transforms ceaselessly among various phase states because of its highly nonlinear and large uncertainty, such as uniform flow with no jam, jammed flow of the kink density wave, and jammed flow of the chaotic density wave.[11,12] Chaos can be found in traffic flow and chaotic phenomena have been reported in traffic patterns. Traffic jams, chaos, and pattern formation are typical signatures of the complex behavior of a traf-

*Project supported by the National Natural Science Foundation of China (Grant No. 50478088) and the Natural Science Foundation of Hebei Province, China (Grant No. E2015202266).

†Corresponding author. E-mail: pmbpgy@hebut.edu.cn

‡Corresponding author. E-mail: Hym127441@163.com

© 2018 Chinese Physical Society and IOP Publishing Ltd

fic system. A chaotic traffic jam means that the density wave traffic jams become unstable, break up, and coalesce irregularly. Any control method that can make traffic flow stable and orderly, and also reduce the uncertainty of traffic flow can be regarded as an effective way to reduce the chaos of traffic flow. If the chaos of traffic flow is identified in time and the chaos control signal is inputted promptly, then traffic systems can transit from disorder states to periodic states.[13,14] In other words, the characteristics of traffic flow and flux on an urban expressway can be varied by appropriately regulating the inflow from the on-ramps to the expressway mainline to achieve a stable equilibrium, and to avoid instabilities and chaos of the system. In terms of controlling a roadway with uninterrupted traffic flow, chaos control with only one on-ramp section and some controller-optimized design is yet to be reported, such as partial facing a coordinated control section on a freeway with only one on-ramp segment and a mainline segment.[15,16] Typical devices for chaos control can improve traffic states, suppress traffic jamming, and enhance traffic operating efficiency have been proven by previous research.[15–17] However, few approaches are related to complex networks and their synchronization. A large-scale coordinated control section has not been discussed. Therefore, it is necessary to study chaos control in application to traffic control on a expressway.

Complex networks are a typical type of complex systems, representing the complex interactions among different components.[18–22] Synchronization is one of the typical collective behaviors of complex networks, which means that the states of a system reach some identical values or asymptotic trajectories.[23] In all of these control methods, pinning control, in which only partial nodes are used to input the control signal, has been widely investigated to save control costs.[24–27] If we use the pinning nodes as the subsystems to which the metering signals are inputted and synchronization as our direct control objective, then the method of pinning control is the same as that of multi-ramp coordinated metering. The road's operating efficiency may be optimized at small control cost if the system is in a synchronization state. Consequently, three patterns are defined for the link of the concrete section on urban expressway and a node coupling model is established by using cell transmission model (CTM). We have designed a pinning chaos controller corresponding to multi-ramp coordinated controller, whose objective is to minimize the errors between the traffic densities and the delayed ones to control chaos by using the delayed feedback control (DFC) method. The concrete pinning chaos control nodes can be obtained and the parameters of the controller are optimized by using the stability theory of complex networks. The correctness and effectiveness of this method are verified in a simulation example.

This paper is divided into five sections. The node coupling model of urban expressway based on complex networks is established by using CTM in Section 2. The chaos controller design is presented in Section 3. A simulation example is presented in Section 4. Finally, the conclusions of the work are summarized in Section 5.

2. Node coupling model of an urban expressway based on complex networks

2.1. CTM of an urban expressway

An urban expressway is divided into N cells and there are three types of cells, as follows: mainline cell, on-ramp cell, and off-ramp cell. To describe the actual traffic flow processing of the studied object, we established an improved CTM,[28,29] where the length of each cell that may be different and the length of cell m is l_m. Considering that there are three types of segments on the urban expressway, three types of connections were defined in the CTM, as shown in Fig. 1, where simple connection exists in basic segment, fused connection exists in confluence segment, and separate connection exists in distributary segment. $S_{m-1}(t)$ and $S_p(t)$ denote the numbers of vehicles that can move from mainline cell $m-1$ and on-ramp cell p to mainline cell m at discrete time step t, respectively. $f_{m-1,m}(t)$ and $f_{p,m}(t)$ denote the numbers of vehicles moving from mainline cell $m-1$ and on-ramp cell p to mainline cell m at step t, respectively. $f_{m-1,o}(t)$ denotes the number of vehicles moving from mainline cell $m-1$ to off-ramp cell o at step t. The numbers of vehicles for mainline cell m and off-ramp o that they can be accepted at step t are $R_m(t)$ and $R_o(t)$, respectively. $Q_m(t)$ denotes the capacity of cell m. v is the free flow speed and ω is the backward propagation of the crowded wave velocity. $k_m(t)$ represents the density of mainline cell m at step t. The congestion density is K_J. α denotes the fuse ratio of on-ramp p to mainline cell and β denotes the separation ratio between off-ramp cell and mainline cell.

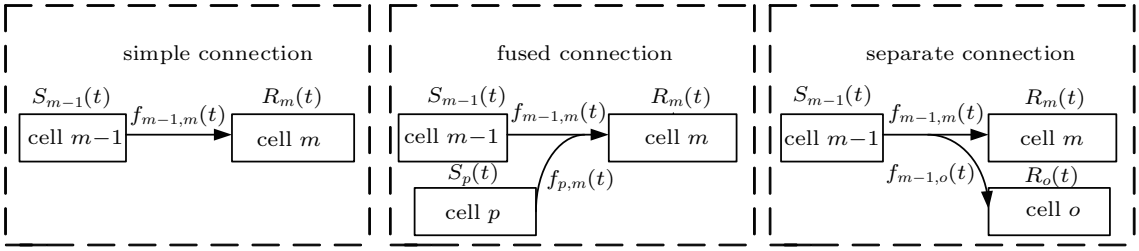


Fig. 1. Transmission relation in three types of connections.

Flow conservation for simple connection is expressed by the following equations:

$$f_m(t) = f_{m-1,m}(t) = \min\{S_{m-1}(t), R_m(t)\}, \quad (1)$$

$$S_{m-1}(t) = \min\{vk_{m-1}(t), Q_{m-1}(t)\}, \quad (2)$$

$$R_m(t) = \min\{Q_m(t), w(K_J - k_m(t))\}, \quad (3)$$

where $f_m(t)$ denotes the flow of vehicles into cell m at step t. Equation (1) indicates that the number of vehicles for a mainline cell moving from its upstream cell is equal to the minimal value between the number of vehicles that can move from its upstream cell and the number of vehicles that can be accepted.[29] Equation (2) indicates that the number of vehicles for a mainline cell that can move to its downstream cell is not larger than the capacity of the cell. Equation (3) indicates that the number of vehicles that a cell can be accepted is equal to the minimal value between the capacity of the cell and the number of its remaining vehicles.

Flow conservation for fused connection is expressed by the following equations:

$$f_m(t) = f_{m-1,m}(t) + f_{p,m}(t) = \begin{cases} S_{m-1}(t) + S_p(t), & R_m(t) > S_{m-1}(t) + S_p(t), \\ \text{med}\{S_{m-1}(t), R_m(t) - S_p(t), (1-\alpha)R_m(t)\} & \\ +\text{med}\{S_p(t), R_m(t) - S_{m-1}(t), \alpha R_m(t)\}, & R_m(t) \le S_{m-1}(t) + S_p(t), \end{cases} \quad (4)$$

where function med denotes take median of three items.[29] Equation (4) indicates that all vehicles can move from cell $m-1$ and on-ramp cell p to cell m if cell m has sufficient space for acceptance, otherwise there will be a certain proportion for $f_{m-1,m}(t)$ and $f_{p,m}(t)$,

Flow conservation for separate connection is expressed by the following equations:

$$f_{m-1,m}(t) = (1-\beta)\min\{S_{m-1}(t), R_m(t)/(1-\beta), R_o(t)/\beta\}, \quad (5)$$

$$f_{m-1,o}(t) = \beta \min\{S_{m-1}(t), R_m(t)/(1-\beta), R_o(t)/\beta\}. \quad (6)$$

Equations (5) and (6) indicate that vehicles can move from cell $m-1$ to cell m and off-ramp cell o if they have sufficient spaces for acceptance, otherwise there will be a certain proportion for $f_{m-1,m}(t)$ and $f_{m-1,o}(t)$.[29]

For mainline cell m, which has three types of connections, the state transfer equation of flux is described as follow:

$$q_m(t+1) = q_m(t) + f_m(t) - f_{m,m+1}(t) - f_{m,o}(t). \quad (7)$$

Equation (7) indicates that the number of vehicles in a cell is equal to its number at the previous simulation step plus the number of vehicles from its upstream cell and on-ramp cell, and minus the number of vehicles that move to its downstream cell and off-ramp cell. For a mainline cell with only one or two types of connections, we set the number of moving vehicles be zero at the direction without adjacent cell.

2.2. Node coupling model of urban expressway based on complex networks

Considering the particularity of urban expressway, we use a normal subsystem as shown in Fig. 2 as a node, which consists of a mainline cell, an on-ramp cell, and an off-ramp cell. Each node is only connected with two adjacent nodes, just as each subsystem of urban expressway is only connected to its upstream and downstream. For other types of nodes, we set the flux of on-ramp to be zero for the subsystem without on-ramp, the flux of off-ramp to be zero for the subsystem without off-ramp, and the flux of on-ramp and off-ramp to be zero for the only mainline subsystem. The urban expressway consists of N nodes, where an overpass is divided into four types of nodes according to the concrete component.

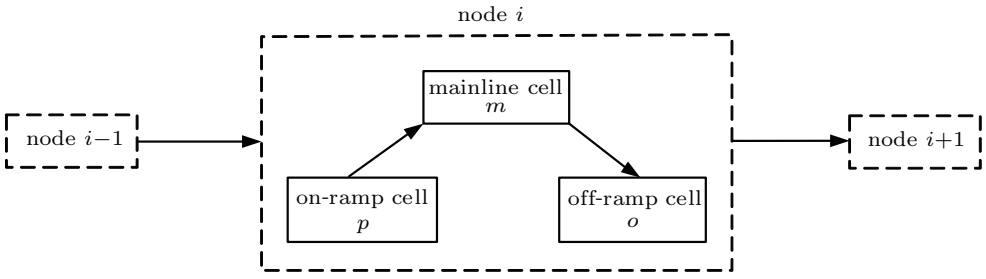


Fig. 2. Sketch of normal node.

Obviously, the state transfer equation of flux for mainline cell m of node i can be described by Eq. (7). For node i, the number of accepted vehicles for cell m of node i at step t is $R_{i,m}(t)$. The number of vehicles moving from cell m is $S_{i,m}(t)$. The number of vehicles moving from on-ramp cell p of node i is $S_{i,p}(t)$. Here we assume that the number of vehicles moving from on-ramp p to mainline cell m is within the permissible range $\alpha R_{i,m}(t)$, the number of vehicles moving from on-ramp

p to mainline cell m is $\min\{S_{i,p}(t), aR_{i,m}(t)\}$. In addition, we assume that the reception capacity of off-ramp cell o is infinite; that is, the number of vehicles moving from the mainline cell m to off-ramp o is $\beta S_{i,m}(t)$. According to Eq. (7), the state transfer equation of flux for mainline cell m of node i is described as follows:

$$\begin{aligned} q_m(t+1) &= q_m(t) + \min\{S_{i,p}(t), \alpha R_{i,m}(t)\} \\ &\quad - \beta S_{i,m}(t) + f_{i-1,i}(t) - f_{i,i+1}(t), \\ &\quad i = 1,2,\ldots,N, \end{aligned} \tag{8}$$

where $f_{i-1,i}(t)$ and $f_{i,i+1}(t)$ represent the numbers of vehicles moving from node $i-1$ to i and from node i to $i+1$ at step t, respectively. Equation (8) indicates that the number of vehicles for a cell at the next step is equal to the number at the present step plus the number of vehicles from its upstream cell and on-ramp cell, and minus the number of vehicles that move to its downstream cell and off-ramp cell.

Here we use $k_{i,m}(t)$, which represents the traffic density of mainline cell m of node i, as the state variable of node i. l_i represents the product of the mainline cell length of node i and the number of lanes. The state transfer equation of density for node i called node coupling model of urban expressway can be derived as follows if equation (8) is divided by l_i on both sides:

$$\begin{aligned} k_{i,m}(t+1) &= k_{i,m}(t) + [\min\{S_{i,p}(t), \alpha R_{i,m}(t)\} - \beta S_{i,m}(t)]\frac{\varepsilon}{l_i} \\ &\quad + [f_{i-1,i}(t) - f_{i,i+1}(t)]\frac{\varepsilon}{l_i} \\ &= f(k_{i,m}(t)) + [f_{i-1,i}(t) - f_{i,i+1}(t)]\frac{\varepsilon}{l_i}, \\ &\quad i = 1,2,\ldots,N, \end{aligned} \tag{9}$$

where $f(k_{i,m}(t))$ denotes the internal state vector of node i at t and ε denotes the simulation step.

Considering that many of the urban expressways in China are ring networks, we used a ring network as the concrete studied objective, the state transfer equation of Eq. (9) for node i called node coupling model of urban expressway can be derived as follows:

$$k_{i,m}(t+1) = f(k_{i,m}(t)) + a\sum_{j=1}^{N} b_{ij}k_j(t), \ i = 1,2,\ldots,N, \tag{10}$$

$$\boldsymbol{B} = (b_{ij})^{N\times N} = \begin{bmatrix} -2 & 1 & 0 & \cdots & 1 \\ 1 & -2 & 1 & \cdots & 0 \\ 0 & 1 & -2 & \cdots & 0 \\ \cdots & \cdots & \cdots & \ddots & \cdots \\ 1 & 0 & \cdots & 1 & -2 \end{bmatrix}, \tag{11}$$

$$k_j(t) = [f_{j-1,j}(t) - f_{j,j+1}(t)]\frac{\varepsilon}{l_i}, \tag{12}$$

where $a\sum_{j=1}^{N} b_{ij}k_j(t)$ represents the coupling relationship between nodes i and j. The matrix $\boldsymbol{B} = (b_{ij})^{N\times N} \in \mathrm{R}^{N\times N}$ in Eq. (11) represents the adjacency configuration of the networks. If there is a connection between nodes i and j ($i \neq j$), then $b_{ij} = b_{ji} = 1$, otherwise, $b_{ij} = b_{ji} = 0$ ($i \neq j$). Diagonal elements are $b_{ii} = -\sum_{j=1,j\neq i}^{N} b_{ij} = -\sum_{j=1,j\neq i}^{N} b_{ji} = -c_i$, $i = 1,2,\ldots,N$, where c_i denotes the degree of node i. Transmission relations of three connections are considered among mainline cell, on-ramp cell, and off-ramp cell. The coupling strength is a, where $a = 1$ in Eq. (10). As the nearest neighbor complex networks, each node of urban expressway is only connected to its downstream node and upstream node. So, except for the main diagonal elements, the matrix $\boldsymbol{B}$ only has two nonzero elements.

3. Design of a coordinated chaos controller

3.1. Chaos control principle

To simplify the problem, only the mode of multi-on-ramp coordinated control was studied. By using the information gathering facilities and relating data processing, the parameters of traffic flow for each node (e.g., traffic volume, traffic density, average velocity, time headway, and on-ramp queue length, etc.) are gathered and computed. After having extracted the features vector of time series data for traffic flow as the input variables, we can compute the maximum Lyapunov exponent ($\lambda_{\max}$) of each node.[15,16] If $\lambda_{\max}$ of each node is not larger than zero, the system is not in a chaotic state, meaning that the system is in ordered motion. No on-ramp metering signal is inputted, otherwise the system is in a chaotic state. The coordinated chaos control signals will be input in the next step. After the control signals have been input many steps, $\lambda_{\max}$ of each node possesses negative values continuously. The traffic flow resumes ordered motion; that is, it is not in a chaotic state. The coordinated on-ramp metering control signals will be input continuously in the next 5 or 10 steps to maximize the effectiveness of control. We then cancel the coordinated on-ramp metering signals.

3.2. Pinning chaos control model using DFC

The DFC mechanism proposed by Pyragas is the most important method of chaos control,[30,31] in which the unknown unstable periodic orbits (UPO) are estimated by a time-delayed state. The feedback used in the control strategy is based on the difference between the current state of the system and a time-delayed one. The delay constant is chosen to be equal to the period of the target UPO, which is assumed to be known a priori. As such, the DFC method is also referred to as the time-delayed feedback control or time-delayed autosynchronization method. From the viewpoint of experimental physics, DFC does not need to model the internal dynamics of the object to be controlled. Therefore, it can be easily implemented in the chaos control of many complex uncertain

systems, particularly to social and economic systems; for example, the traffic system. So we use DFC as the coordinated chaos control method of an urban expressway. To save control cost discussed in Section 1, only partial nodes are inputted as coordinated control signals or added as control variables. The controlled nodes are called pinning nodes. The state transfer equation of the urban expressway in Eq. (10) is revised as follows:

$$\begin{aligned} k_{i,m}(t+1) &= f(k_{i,m}(t)) + a\sum_{j=1}^{N} b_{ij}k_j(t) + u_i(t), \\ & i = 1,2,\ldots,N, \end{aligned} \tag{13}$$

where

$$u_i(t) = -a\sum_{i=1}^{N} d_i(k_{i,m}(t-1) - k_{i,m}(t)). \tag{14}$$

Here the control variable $u_i(t)$ represents the adjusted value of density for node i. This can be realized by the inflow regulating of on-ramp. The feedback gain $d_i > 0$ if $i = 1,2,\ldots,g$ and $d_i = 0$ if $i = g+1,g+2,\ldots,N$, where g represents the number of pinning control nodes, the method is called pinning chaos control if $g < N$, otherwise it is called global chaos control. In particular, the method is called an on-ramp control if $g = 1$, where the ALINEA algorithm is a classic one.

Define the error of node i as

$$e_i(t) = k_i(t-1) - k_i(t), \quad i = 1,2,\ldots,N. \tag{15}$$

Then, the errors can be described as

$$e_i(t+1) = k_i(k) - f(k_i(t)) - a\sum_{j=1}^{N} b_{ij}e_j(t) + a\sum_{i=1}^{N} d_i e_i(t). \tag{16}$$

If the errors tend to zero, then the urban expressway described in Subsection 2.2 will stabilize and achieve synchronization.

3.3. Synchronization criterion of urban expressway

Before stating the main results of this paper, some preliminaries need to be given for convenient analysis.

Assumption 1 There is a constant θ that makes the nonlinear function $\boldsymbol{f}(\boldsymbol{k}(t))$ in the network of urban expressway satisfy

$$\boldsymbol{f}(\boldsymbol{k}(t)) \geq \theta\boldsymbol{k}(t-1). \tag{17}$$

Lemma 1 (Schur complement)[32] The following linear matrix inequality (LMI)

$$\begin{pmatrix} \boldsymbol{Q}(x) & \boldsymbol{S}(x) \\ \boldsymbol{S}^{\mathrm{T}}(x) & \boldsymbol{R}(x) \end{pmatrix} > 0 \tag{18}$$

is equivalent to one of the following conditions:

$$\begin{cases} \boldsymbol{Q}(x) > 0,\ \boldsymbol{R}(x) - \boldsymbol{S}^{\mathrm{T}}(x)\boldsymbol{Q}^{-1}(x)\boldsymbol{S}(x) > 0, \\ \boldsymbol{R}(x) > 0,\ \boldsymbol{Q}(x) - \boldsymbol{S}(x)\boldsymbol{R}^{-1}(x)\boldsymbol{S}^{\mathrm{T}}(x) > 0, \end{cases} \tag{19}$$

where $\boldsymbol{Q}(x) = \boldsymbol{Q}^{\mathrm{T}}(x)$, $\boldsymbol{R}(x) = \boldsymbol{R}^{\mathrm{T}}(x)$.

Theorem 1 If the matrix satisfies the following conditions:

$$\begin{bmatrix} (\theta^2-1)\boldsymbol{I}_N + a\theta(\boldsymbol{B}-\boldsymbol{D}) + a\theta(\boldsymbol{B}-\boldsymbol{D})^{\mathrm{T}} & a(\boldsymbol{B}-\boldsymbol{D}) \\ a(\boldsymbol{B}-\boldsymbol{D})^{\mathrm{T}} & -\boldsymbol{I}_N \end{bmatrix} < 0, \tag{20}$$

the network of urban expressway described in Subsection 2.2 will stabilize and achieve synchronization, where $\boldsymbol{D} = \mathrm{diag}(d_1,d_2,\ldots,d_g,0,\ldots,0)$.

Proof Construct a Lyapunov function $V(t) = \boldsymbol{e}^{\mathrm{T}}(t)\boldsymbol{e}(t)$, and use formulas (13)–(16), then

$$\begin{aligned} \Delta V(t) &= V(t+1) - V(t) \\ &= \boldsymbol{e}^{\mathrm{T}}(t+1)\boldsymbol{e}(t+1) - \boldsymbol{e}^{\mathrm{T}}(t)\boldsymbol{e}(t) \\ &= [\boldsymbol{k}(t) - \boldsymbol{k}(t+1)]^{\mathrm{T}}[\boldsymbol{k}(t) - \boldsymbol{k}(t+1)] - \boldsymbol{e}^{\mathrm{T}}(t)\boldsymbol{e}(t), \\ &= [\boldsymbol{k}(t) - \boldsymbol{f}(\boldsymbol{k}(t)) - a\boldsymbol{B}\boldsymbol{e}(t) + a\boldsymbol{D}\boldsymbol{e}(t)]^{\mathrm{T}} \\ &\quad \times [\boldsymbol{k}(t) - \boldsymbol{f}(\boldsymbol{k}(t)) - a\boldsymbol{B}\boldsymbol{e}(t) + a\boldsymbol{D}\boldsymbol{e}(t)] \\ &\quad - \boldsymbol{e}^{\mathrm{T}}(t)\boldsymbol{e}(t). \end{aligned} \tag{21}$$

By using Assumption 1, we have

$$\begin{aligned} \Delta V(t) &\leq [\theta\boldsymbol{k}(t) - \theta\boldsymbol{k}(t-1) - a\boldsymbol{B}\boldsymbol{e}(t) + a\boldsymbol{D}\boldsymbol{e}(t)]^{\mathrm{T}}[\theta\boldsymbol{k}(t) - \theta\boldsymbol{k}(t-1) - a\boldsymbol{B}\boldsymbol{e}(t) + a\boldsymbol{D}\boldsymbol{e}(t)] - \boldsymbol{e}^{\mathrm{T}}(t)\boldsymbol{e}(t) \\ &= [\theta\boldsymbol{e}(t) + a\boldsymbol{B}\boldsymbol{e}(t) - a\boldsymbol{D}\boldsymbol{e}(t)]^{\mathrm{T}}[\theta\boldsymbol{e}(t) + a\boldsymbol{B}\boldsymbol{e}(t) - a\boldsymbol{D}\boldsymbol{e}(t)] - \boldsymbol{e}^{\mathrm{T}}(t)\boldsymbol{e}(t) \\ &= [\theta\boldsymbol{e}^{\mathrm{T}}(t) + a\boldsymbol{e}^{\mathrm{T}}(t)\boldsymbol{B}^{\mathrm{T}} - a\boldsymbol{e}^{\mathrm{T}}(t)\boldsymbol{D}^{\mathrm{T}}][\theta\boldsymbol{e}(t) + a\boldsymbol{B}\boldsymbol{e}(t) - a\boldsymbol{D}\boldsymbol{e}(t)] - \boldsymbol{e}^{\mathrm{T}}(t)\boldsymbol{e}(t) \\ &= \theta^2\boldsymbol{e}^{\mathrm{T}}(t)\boldsymbol{e}(t) + a\theta\boldsymbol{e}^{\mathrm{T}}(t)\boldsymbol{B}\boldsymbol{e}(t) - a\theta\boldsymbol{e}^{\mathrm{T}}(t)\boldsymbol{D}\boldsymbol{e}(t) + a\theta\boldsymbol{e}^{\mathrm{T}}(t)\boldsymbol{B}^{\mathrm{T}}\boldsymbol{e}(t) + a^2\boldsymbol{e}^{\mathrm{T}}(t)\boldsymbol{B}^{\mathrm{T}}\boldsymbol{B}\boldsymbol{e}(t) \\ &\quad - a^2\boldsymbol{e}^{\mathrm{T}}(t)\boldsymbol{B}^{\mathrm{T}}\boldsymbol{D}\boldsymbol{e}(t) - a\theta\boldsymbol{e}^{\mathrm{T}}(t)\boldsymbol{D}^{\mathrm{T}}\boldsymbol{e}(t) - a^2\boldsymbol{e}^{\mathrm{T}}(t)\boldsymbol{D}^{\mathrm{T}}\boldsymbol{B}\boldsymbol{e}(t) + a^2\boldsymbol{e}^{\mathrm{T}}(t)\boldsymbol{D}^{\mathrm{T}}\boldsymbol{D}\boldsymbol{e}(t) - \boldsymbol{e}^{\mathrm{T}}(t)\boldsymbol{e}(t) \\ &= \boldsymbol{e}^{\mathrm{T}}(t)[(\theta^2-1)\boldsymbol{I}_N + a\theta(\boldsymbol{B}-\boldsymbol{D}) + a\theta(\boldsymbol{B}-\boldsymbol{D})^{\mathrm{T}} + a^2(\boldsymbol{B}-\boldsymbol{D})(\boldsymbol{B}-\boldsymbol{D})^{\mathrm{T}}]\boldsymbol{e}(t) \\ &= \boldsymbol{e}^{\mathrm{T}}(t)\begin{bmatrix} (\theta^2-1)\boldsymbol{I}_N + a\theta(\boldsymbol{B}-\boldsymbol{D}) + a\theta(\boldsymbol{B}-\boldsymbol{D})^{\mathrm{T}} & a(\boldsymbol{B}-\boldsymbol{D}) \\ a(\boldsymbol{B}-\boldsymbol{D})^{\mathrm{T}} & -\boldsymbol{I}_N \end{bmatrix}\boldsymbol{e}(t). \end{aligned} \tag{22}$$

We can then obtain Eq. (20) by using Lemma 1.

Remark 1 According to Assumption 1 and Lemma 1, if a network is given, then the stable condition is determined by Eq. (20), which is determined by the coupling strength a, the adjacency matrix $\boldsymbol{B}$, and the feedback gain matrix $\boldsymbol{D}$ of the network. An appropriate θ and $\boldsymbol{D}$ may make Theorem 1 hold. Considering the particularity of urban expressway, we choose to input the control signal on the on-ramp of the upstream nodes. We set the number of control nodes from 1 to N until the feasible solution in Eq. (20) can be calculated by using LMI toolbox in Matlab. We then obtain the pinning nodes and $\boldsymbol{D}$, where the pinning number is the smallest. It is concluded that such a weighted complex dynamical network can be pinned to its equilibrium by using some controllers. Therefore, the goal of locally asymptotically stable for urban expressway can be achieved.

4. Simulation results and discussion

4.1. Application background

The clockwise direction of the northwest half-ring Tianjin City Expressway in China, which is shown in Fig. 3, was used as the studied objective, where the length of the one-way four-lane mainline is 20 km. The numbers of on-ramp and off-ramp in the urban expressway are 15 and 17, respectively. Each ramp is numbered, where p and o represent on-ramp and off-ramp, respectively. According to traffic survey and design information of the urban expressway, the maximal flow of urban expressway $Q = 1800$ veh/(h·lane), free flow velocity $v = 60$ km/h, backward wave velocity $\omega = 20$ km/h, critical density $k_c = 45$ veh/(km·lane), and congestion density $K_J = 110$ veh/(km·lane). The vehicles consist mainly of cars and large vehicles, where the proportion of cars is 0.88. Traffic congestion is particularly severe during rush hour.

Using the rules of Section 2 and considering the concrete geometric alignment of the expressway, the studied objective in Fig. 3 is divided into 16 mainline cells, 15 on-ramp cells, and 17 off-ramp cells. Each ramp corresponds to a ramp cell and its length is that of its ramp cell. Each mainline cell starts from the weaving segment between one ramp and the mainline and ends at the starting point of its downstream mainline cell. The length of a mainline cell is the distance from its starting point to the ending point. The system consists of 16 nodes and each node from upstream to downstream is marked to the number from 1 to 16 in the clockwise direction, where each node only includes a mainline cell. Table 1 shows the length of mainline cell of each node and the concrete ramps that the node contains and the starting and ending points of each node, where the concrete ramps number that a node contains may be different due to the uneven distribution of the ramps. In the simulation, the desired density $\bar{k} = 42$ veh/(km·lane) and the duration of each time step is 10 s. To display the control effect, we assume that queue in each on-ramp is out of constrained. The first 360 time steps are discarded to avoid transient behavior. The results described in this paper are obtained after 360 time steps.

To test the validities of the proposed models and identify the relevant parameters, some comparisons of the phase diagrams of the actual statistics data and the simulation results for the CTMs of all nodes and the node coupling model of the studied objective were made. Figure 4 shows a comparison of flow-density in macroscopic phase diagram for the studied section of the urban expressway. Obviously, the two fitting curves are basically the same. There is a similar comparison diagram between the actual statistics data of the node and the simulation result for each node. Therefore, the validity is preliminarily proved.

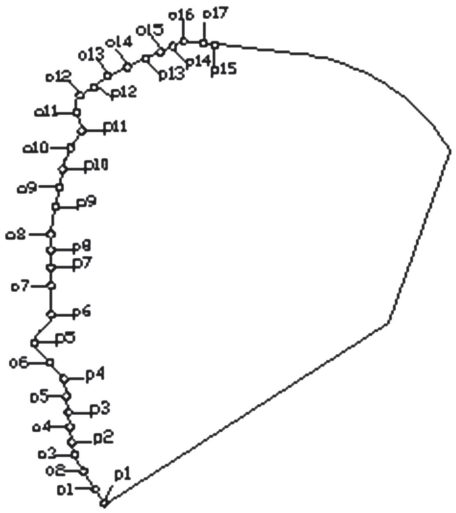


Fig. 3. Topology diagram of the northwest semicircular Tianjin City Expressway.

Table 1. Mainline cell lengths of nodes and their containing ramps.

Node	1	2	3	4	5	6	7	8
Mainline cell length/km	1.00	1.08	0.68	0.75	0.93	2.10	1.90	1.00
Containing ramps	$p1$,$o1$	$p2$,$o2$,$o3$	$p3$,$o4$	$p4$,$o5$	$p5$,$o6$	$p6$,$o7$	$p7$	$p8$,$o8$
Starting and ending points	$p1$,$o2$	$o2$,$o4$	$o4$,$o5$	$o5$,$o6$	$o6$,$p6$	$p6$,$p7$	$p7$,$p8$	$p8$,$p9$
Node	9	10	11	12	13	14	15	16
Mainline cell length/km	1.20	1.60	1.20	1.30	1.25	0.93	1.60	0.67
Containing ramps	$p9$,$o9$	$p10$,$o10$	$p11$,$o11$	$p12$,$o12$	$o13$,$o14$	$p13$,$o15$	$p14$,$o16$	$p15$,$o17$
Starting and ending points	$p9, p10$	$p10, p11$	$p11, o12$	$o12, o13$	$o13, p13$	$p13, p14$	$p14, o17$	$o17, p1$ 5

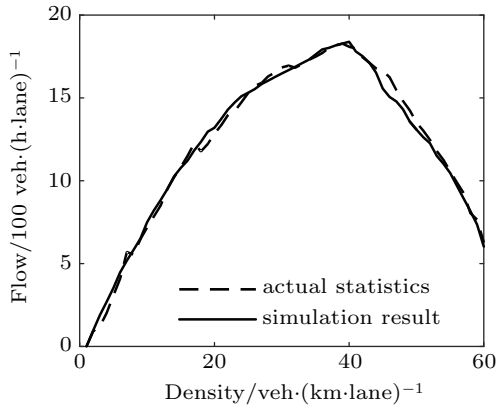


Fig. 4. Comparison of phase diagram between the actual statistics and the simulation result.

4.2. Effect analysis of chaos control using the proposed control method

The clockwise direction of the northwest half-ring Tianjin City Expressway from 7:00 am to 8:00 am was used as our experiment site and time period. According to the traffic survey, we can obtain the traffic flow with time-dependent characteristics. Table 2 shows the intervals of on-ramp demand and off-ramp flow for partial nodes during the time period. Through the statistics and the related calculation, the combined ratio α and the separation ratio β are set to 0.4 and 0.3, respectively. Figure 5 shows the fluctuations of density and $\lambda_{\max}$ for nodes 6–8 in a case from step 50 to 150, where no-control signal (NCS) and the proposed pinning chaos control signal (PCC) are inputted, respectively. In the case, $\lambda_{\max}$ of node 8 at step 53 is 0.000076, meaning that it is larger than 0 and the coordinated chaos control signal needs to be inputted. By using the PCC method and setting $\theta = 0.94$, we obtain the pining number of 3, meaning that the inflows of on-ramps from nodes 6–8 need to be regulated. The obtained feedback gains are $d_8 = 0.1496$, $d_7 = 0.1230$, $d_6 = 0.1496$. The pinning chaos control signals were then inputted after two steps. Table 3 shows the comparison of flux and total travel time (TTT) by using NCS and PCC, respectively, where the flux represents the total number of vehicle moving from the studied objective per hour, and TTT is defined as follow:[33]

$$\mathrm{TTT} = \varepsilon \sum_{j=1}^{g} \sum_{i=1}^{N} l_i k_i (t + j). \tag{23}$$

Table 2. Intervals of on-ramp demand and off-ramp flow for partial nodes.

Node	15	13	11	9	8	6	5
On-ramp demand/(veh/h)	[720,840]	[900,1080]	[1380,1680]	[1500,1800]	[720,800]	[840,960]	[1680,1740]
Off-ramp flow/(veh/h)	[480,540]	[600,660]	[300,360]	[540,600]	[600,660]	[1260,1320]	[1260,1300]

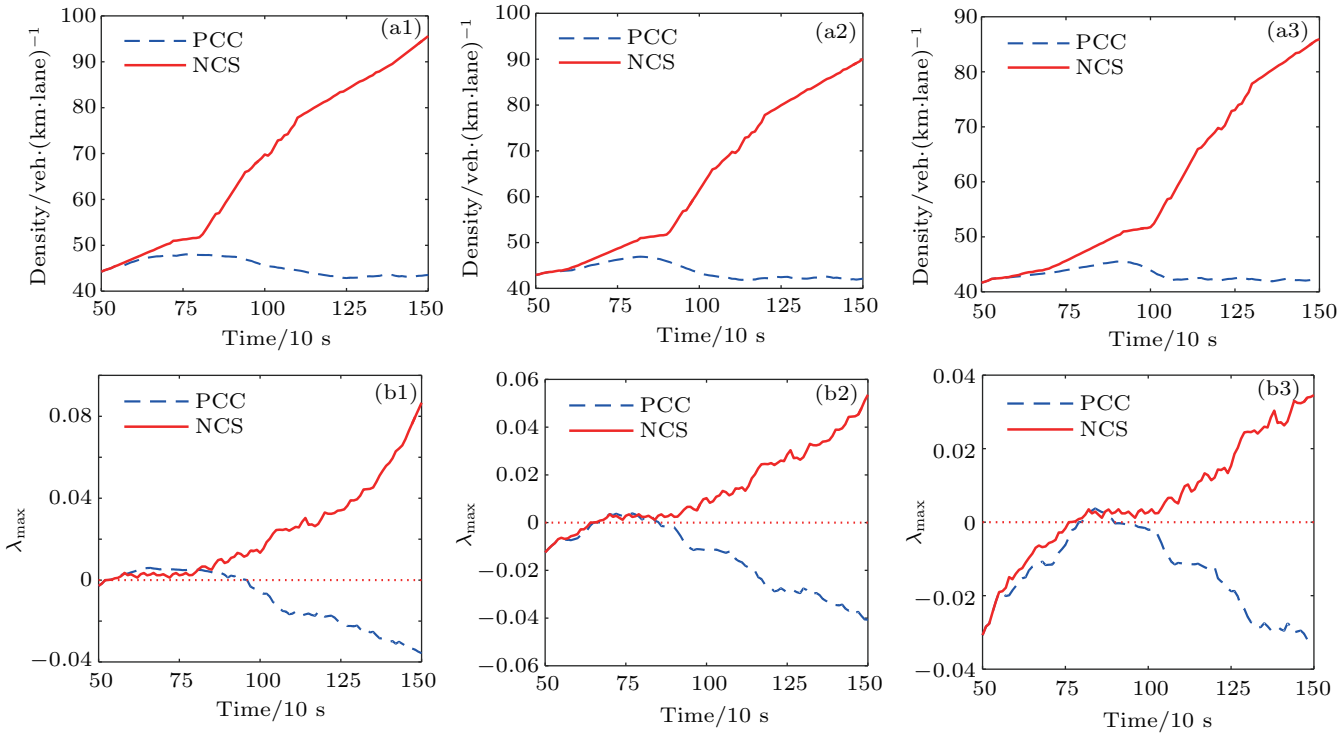


Fig. 5. (color online) The simulation result of (a) density profile and (b) $\lambda_{\max}$ profile using NCS and PCC in a case: (a1) and (b1) node 8, (a2) and (b2) node 7, and (a3) and (b3) node 6.

Table 3. Comparison of TTT and flux by using NCS and PCC.

Control mode	TTT/s	Flux/veh·h^{-1}
NCS	923110	24753
PCC	809371	26934

The findings are as follows.

1) Without coordinated on-ramp metering signal, the traffic jams phenomenon shown in Fig. 5(a1) appears in node 8. The density of node 8 increases from 45 veh/(km·lane) at step 55 to 65 veh/(km·lane) at step 95, and then increases rapidly to 95 veh/(km·lane) at step 150, which eventually causes a jam phenomenon. $\lambda_{\max}$ of node 8 shown in Fig. 5(b1) keeps positive values after step 55. At the same time, the traffic jams phenomenon shown in Fig. 5 spreads rapidly toward upstream nodes especially nodes 7 and 6. For node 7, the density increases from 45 veh/(km·lane) at step 65 to 51 veh/(km·lane) at step 87, and then increases rapidly to 90 veh/(km·lane) at step 150. $\lambda_{\max}$ keeps positive values after step 65. For node 6, the density increases from 46 veh/(km·lane) at step 76 to 51 veh/(km·lane) at step 85, and then increases rapidly to 86 veh/(km·lane) at step 150. $\lambda_{\max}$ keeps positive values after step 76. This means that the operating efficiency of expressway declines and TTT increases. The conclusion is tested again that a wide-moving jam may occur If the traffic flow is in a chaotic state and no chaos control signal is implemented.

2) Using the PCC method, as can be seen from Fig. 5, after 40 steps, 32 steps, and 30 steps of inputting coordinated pining chaos control signal, $\lambda_{\max}$ of each node remains negative. In other words, we can control the traffic flow chaos using 40 steps or 400 s. The validity of chaos control by using PCC for urban expressway is tested. At the same time, the densities of nodes 6–8 keep vary within the range 40–45 veh/(km·lane). Although the unknown unstable fixed point or periodic orbit has not been set, the traffic flow remains ordered motion if DFC is applied once. The validity of suppressing a wide-moving traffic jam by the proposed chaos control method is tested.

3) Using the PCC method, TTT declines from 923110 s to 809371 s, which decreases 12.6% compared to NCS. The flux increases from 24753 veh/h to 26934 veh/h, which is an improvement of 8.8% compared to NCS. The operating efficiency of expressway is enhanced because the characteristics of traffic flow and the flux for urban expressway could be varied by appropriately regulating the inflow from the on-ramp to the mainline. The system will vary from a chaotic state to ordered motion and a wide-moving traffic jam will be suppressed. The vehicles keep moving at a free flow speed. This makes the flux increase and TTT decrease.

4.3. Comparison with other control methods

Four control methods were used: PCC, global chaos control (GCC), pinning control signal (PCS), and CORDIN,[8]

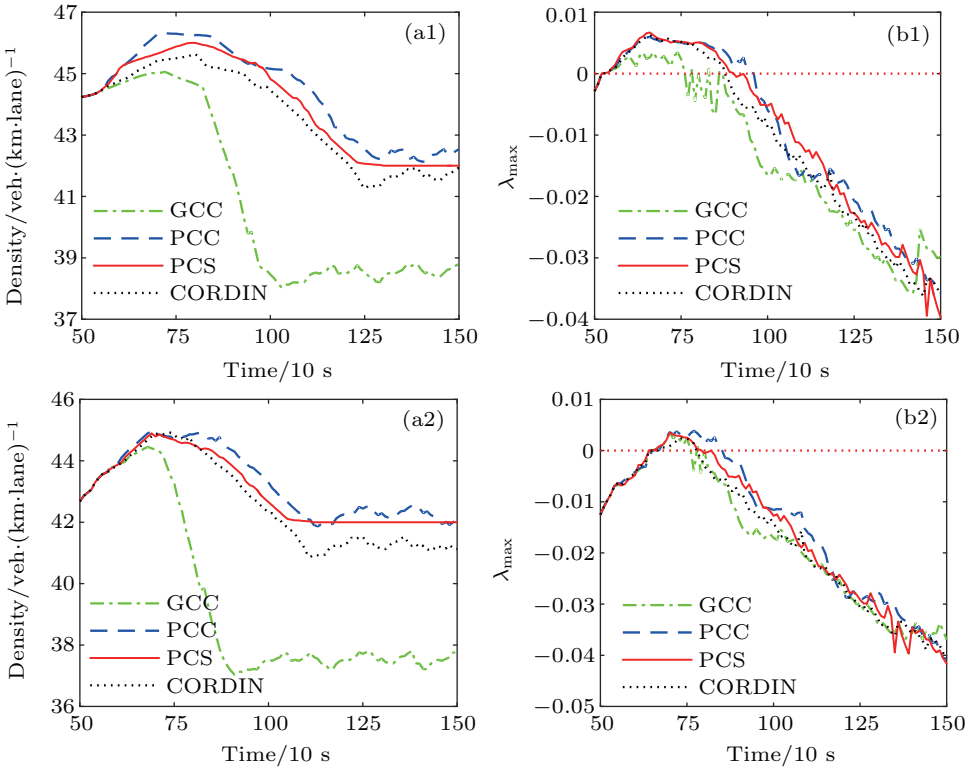


Fig. 6. (color online) The simulation results of (a) density profile and (b) $\lambda_{\max}$ profile using four control methods in a case: (a1) and (b1) node 8, and (a2) and (b2) node 7.

were used to make a comparison. In the PCS method, a small negative neighborhood of critical density is used as the desired density for the condition of inputting a coordinated control signal. $k_i(t-1)$ in Eq. (15) is replaced by the desired density with the same principle and method as PCC, where $k_{\rm d} = 42$ veh/(km·lane). In the GCC method, all nodes are used as control nodes with the same principle and method as PCC. We only select nodes 5–8 to be the control ones in CORDIN, where ALINEA is used as the on-ramp metering algorithm of node 8 and the parameter to be calibrated is $\alpha_1 = 0.7$ for node 7, $\alpha_2 = 0.8$ for nodes 6 and 5. Figure 6 shows the simulation results of density and $\lambda_{\max}$ using four control methods for partial nodes. Figures 7 and 8 show the changes of congestion range for the studied objective and the changes of flux for node 8 using five control methods, respectively. Figure 9 shows the on-ramp queue lengths of partial nodes. Table 4 shows the simulation results of the four indices, where the average queue length of the on-ramps (AQL) is defined as the queue length accumulation of all on-ramps in all simulation steps divided by the number of the on-ramps and the number of simulation steps, and the maximal queue length of the on-ramps (MQL) is defined as the maximum queue length in all on-ramps for all simulation steps. The findings are as follows.

1) As can be seen from Fig. 6, the density of node 8 varies within the range 38–46 veh/(km·lane) from step 55 to 125 after multi-on-ramp metering signals have been input by using GCC method, PCS method, and CORDIN, respectively. The density of node 8 then varies below 42 veh/(km·lane) after step 126. $\lambda_{\max}$ of node 8 varies at first between positive value and

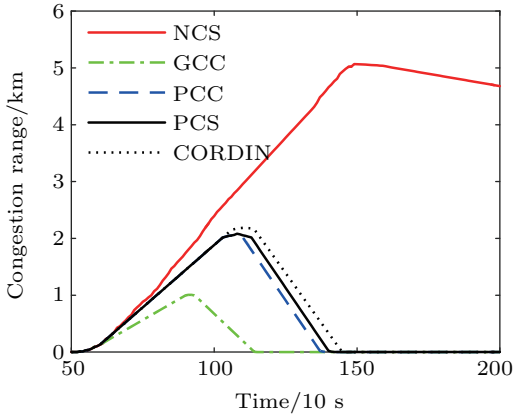


Fig. 7. (color online) Changes of congestion range.

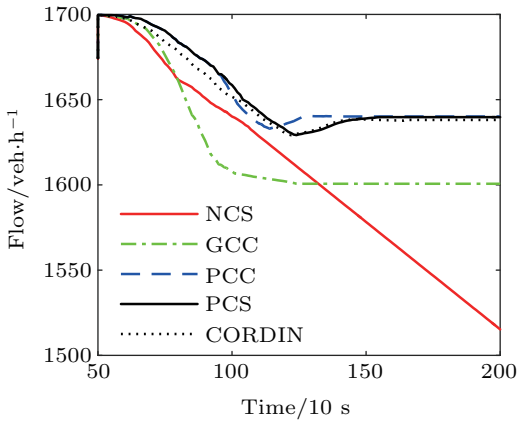


Fig. 8. (color online) Flow changes of node 8.

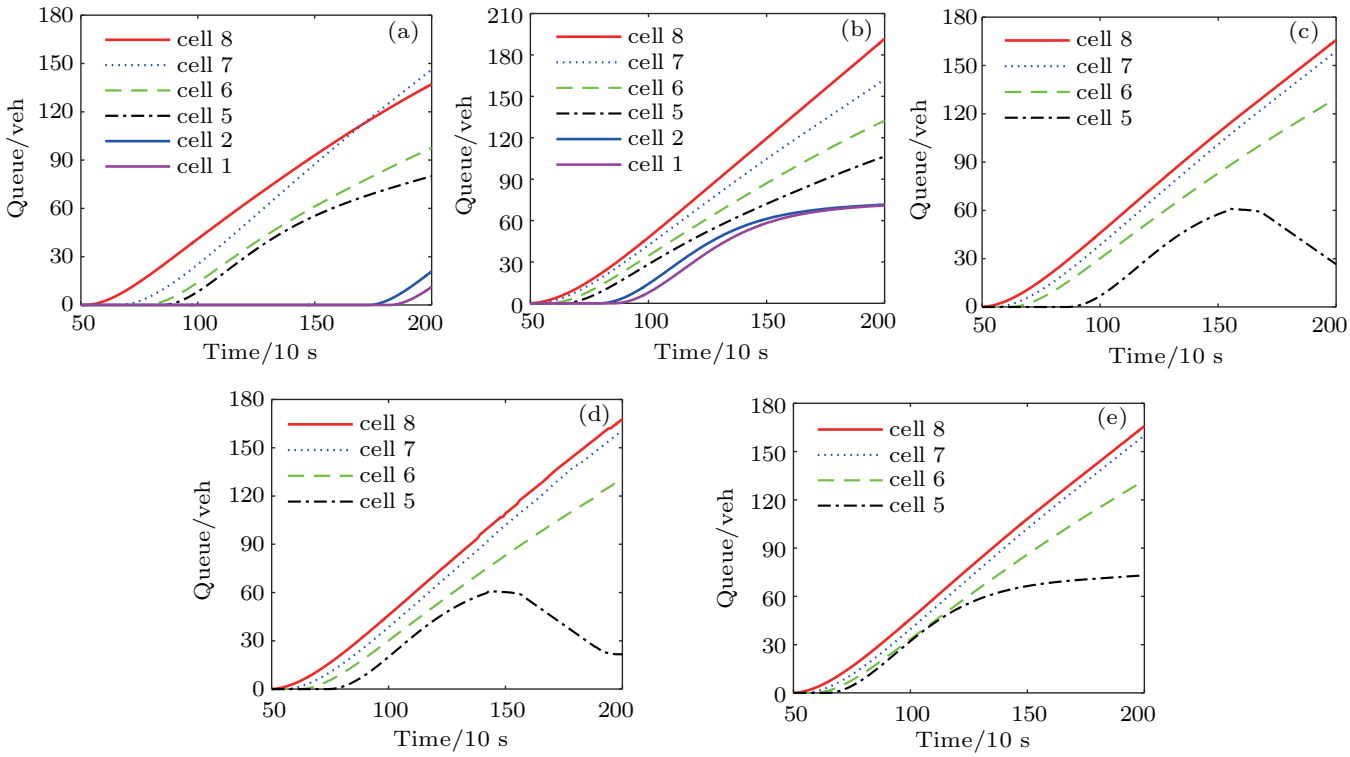


Fig. 9. (color online) On-ramp queue length profiles of partial nodes using coordination control of (a) NCS, (b) GCC, (c) PCC, (d) PCS, and (e) CORDIN.

Table 4. Comparison of four indices among five methods.

Control mode	NCS	PCC	PCS	GCC	CORDIN
TTT/s	923110	806400	806505	877531	809371
Flux/veh·h^{-1}	24753	26934	26915	26052	26656
AQL/veh	25	15	17	23	18
MQL/veh	150	190	191	184	193

negative value, and then remains negative value after multi-on-ramp metering signals have been input 25 steps, 36 steps, and 33 steps, respectively. The same change trend is seen for node 7. The congestion range and duration of the system shown in Fig. 7 decrease greatly and the flux of node 8 shown in Fig. 8 increases. As shown in Table 4, TTT decreases and the flux increases for each control method compared with NCS. A wide-moving jamming phenomenon can be suppressed using each control method. The operating efficiency of urban expressway can be enhanced. At the same time, AQL decreases and MQL does not decrease and perhaps increases for each control method compared with NCS. This happens because the coordinated control signal makes many vehicles that want to travel on the expressway have to travel on the urban streets or queue on the on-ramps. The queue length of some metering on-ramps for each control method may become larger than that with NCS. This creates a problem of social inequity for the ramp users but the average queue length of all on-ramps can be smaller than that with NCS. In addition, the operating efficiency of the urban expressway for all users can be enhanced. The validities of PCS method and GCC method are also proven and the validity of CORDIN is tested again.

2) Using GCC method, the density of node 8 increases at first, it then decreases rapidly, and ultimately keeps varying within the range 37–39 veh/(km·lane). The same change trend is seen for node 7. The TTT for each node is the largest and the flux is the smallest among the four control methods. Assuming that the queue in each on-ramp is out of constraint, the AQL is the largest but the MQL is the smallest among the four control methods. This happens because the expanded control sections or increasing on-ramp metering number make many vehicles that want to travel on the expressway travel instead on ordinary urban streets or queue on the on-ramps. The flux drops due to the restrained traffic demand, although the travel time of most vehicles traveling on the mainline may decline. At the same time, this makes the problem of social inequity for some ramp users more serious. Therefore, the control cost by using GCC method cannot be saved and the operating efficiency is the lowest of the four control methods.

3) Using PCS method, the densities of nodes 8 and 7 increase at first, they then decrease slowly, and ultimately reach 42 veh/(km·lane). Using CORDIN, the densities of nodes 8 and 7 increase at first, they then decrease slowly, and ultimately keep varying within the range 40–42 veh/(km·lane). At the same time, the four control methods have the same change trends of on-ramp queue length, congestion range, and flux for each node, such as nodes 5–8. This happens because PCS is a special method of chaos control, where the desired density is chosen to be the target UPO. The essence of CORDIN, especially in the control goal, is also equal to that of PCS method and PCC method. Therefore, the control effects of the three methods are similar.

4) For the PCC method, TTT is the smallest, the flux is the largest, AQL is the smallest, and MQL is not the best among the four methods. This happens because the PCC method does not need any preliminary knowledge about the target UPO, except for its period. Compared with the PCS method, it can easily be implemented in the chaos control of an uncertain expressway. For CORDIN, its parameters of controllers and the number of control nodes are only determined by the traffic managers rather than by more accurate models and their calculation. The control effect may not be optimal, especially in multi-jamming nodes. Therefore, TTT, the flux, and AQL using the PCC method are the best among the four control methods. Although MQL by using PCC method is not the best and is perhaps the worst among the four control methods, and it makes the problem of social inequity for some ramp users more serious, the operating efficiency of urban expressway for all users can be enhanced. Consequently, the control effect of PCC method is the best among all four control methods.

5. Conclusion

Using CTM, a node coupling model of urban expressway based on complex networks has been established. The pinning chaos controller corresponding to multi-ramp coordinated controller was designed using the DFC method. The synchronization criterion of the system was derived and the feedback gain matrix was obtained. The results of the examples via the simulation experiments indicate its effectiveness. A comparison with other control methods shows the superiority of this method.

This study has observed several limitations. The node coupling model of an urban expressway is still relatively simple and there are several hypotheses in the model. In the simulation case, only a congested node was considered. However, many congested nodes should be discussed. The coordination control, including off-ramp congestion mitigating and combination with urban streets, have not been discussed. Therefore, it is recommended that future studies should concentrated on these problems.

References

[1] Aslani M, Mesgari M S and Wiering M 2017 *Transp. Res. C* **85** 732
[2] Bifulco G N, Cantarella G E, Simonelli F and Velonà P 2016 *Transp. Res. B* **92** 73
[3] Peng G H, Song W, Peng Y J and Wang S H 2014 *Physica A* **398** 76

[4] Haddad J, Ramezani M and Geroliminis N 2013 *Transp. Res. B* **54** 17
[5] Papamichail I, Kotsialos A, Margonis I and Papageorgiou M 2010 *Transp. Res. C* **18** 311
[6] Yang X F, Cheng Y and Chang G L 2018 *Transp. Res. C* **86** 328
[7] Zheng Y M, Cheng R J and Ge H X 2017 *Phys. Lett. A* **381** 2137
[8] Bhouri N, Salem H H and Kauppila J 2013 *Transp. Res. C* **28** 155
[9] Ge H X, Meng X P, Zhu H B and Li Z P 2014 *Physica A* **408** 28
[10] Zhu Z W, Wang H L, Han H C and Xu J 2008 *The 9th International Conference for Young Computer Scientists*, November 2008, Hunan, China, p .2766
[11] Nagatani T 1999 *Phys. Rev. E* **60** 1535
[12] Li K P and Gao Z Y 2004 *Chin. Phys. Lett.* **21** 1212
[13] Jeihani M, James P, Saka A A and Ardeshiri A 2015 *ScienceDirect* **2** 291
[14] Fang Y L and Shi Z K 2015 *Physica A* **422** 40
[15] Pang M B, Ren S S, Wang Y H and Chen P 2013 *J. Highw. Transp. Res. Dev.* **7** 90 (ASCE)
[16] Pang M B, Cai Z H, Yang M and Zhang S S 2015 *J. Highw. Transp. Res. Dev.* **9** 79 (ASCE)
[17] Cheng A Y, Jiang X, Li Y F, Zhang C and Zhu H 2017 *Physica A* **466** 422
[18] Zhang L S, Gu W F, Hu G and Mi Y Y 2014 *Chin. Phys. B* **23** 108902
[19] Song B, Jiang G P, Song Y R and Xia L L 2015 *Chin. Phys. B* **24** 100101
[20] Zhong X, Liu J J, Gao Y and Wu L 2017 *Physica A* **466** 462
[21] Wang Z Y, Hill D J, Chen G and Dong Z Y 2017 *Physica A* **482** 532
[22] Li S B, Wu J J, Gao Z Y, Lin Y and Fu B B 2011 *Acta Phys. Sin.* **60** 050701 (in Chinese)
[23] An X L, Zhang L, Li Y Z and Zhang J G 2014 *Physica A* **412** 149
[24] Wang J A, Nie R X and Sun Z Y 2014 *Chin. Phys. B* **23** 050509
[25] Xu M, Wang J L, Huang Y L, Wei P C and Wang S X 2017 *Neurocomputing* **266** 263
[26] Wang S G and Yao H X 2012 *Chin. Phys. B* **21** 050508
[27] DeLellis P, Garofalo F and Iudice F L 2018 *Automatica* **89** 111
[28] Csikós A and Kulcsár B 2017 *Transp. Res. C* **85** 429
[29] Geng N, Zhao X M, Xie D F, Li X G and Gao Z Y 2015 *Transp. Res. C* **57** 122
[30] Li N, Sun H Y and Zhang Q L 2012 *Chin. Phys. B* **21** 010503
[31] Lee S M, Kwon O M and Park J H 2011 *Chin. Phys. B* **20** 010506
[32] Rakkiyappan R, Sakthivel N and Lakshmanan S 2014 *Chin. Phys. B* **23** 020205
[33] Lu X Y, Varaiya P, Horowitz R, Su D Y and Shladover S E 2011 *Transportation Res. Record* **2229** 55